
CONSTRAINTS IN CAD MODELS FOR REVERSE ENGINEERING USING PHOTOGRAMMETRY

Pierre ERMES

Delft University of Technology, The Netherlands
Faculty of Civil Engineering and Geosciences, Department of Geodesy
p.ermes@geo.tudelft.nl

Working Group V/2

KEY WORDS: CAD, Modeling, Photogrammetry, Reconstruction

ABSTRACT

The paper discusses the use of geometric constraints in a CAD model-based photogrammetric system. The CAD models are represented by CSG (Constructive Solid Geometry) models. The geometric primitives that make up the CSG model are parameterized by their pose and shape parameters. Geometric relations, or constraints, between these primitives are expressed using these parameters.

Constraints can be applied both between the geometric primitives in a CSG model and between CSG models. For example, continuity requirements between two connected piping elements constrain the relative position of the elements as well as their relative orientation.

The constraints are formulated as weighted linearized observation equations and are included in a least-squares adjustment together with the photogrammetric measurements on the edges. The exterior orientation parameters of the images are also estimated in the adjustment.

A pilot project was done on a gas-exploration site. Only the images and a couple of tape measurements were acquired on the site - no markers were used. The model-oriented photogrammetric system, Piper, combines image observation and geometric constraints in a bundle adjustment to reconstruct an accurate CAD model of the installation.

1 INTRODUCTION

An accurate "as-built" model of a piping installation can serve several purposes; such as revamping, inspection and maintenance, and part replacement. Safety regulations may also demand that an up-to-date model of an installation is available. Photogrammetry is an often used technique for the reconstruction of industrial installations (Benning, 1997), (Hilgers et al., 1998), (Jones et al., 1996).

Industrial installations are usually built with standardized components for economic reasons. CAD models of these components are available in large databases or catalogs. It appears that most standardized components can be modeled with only a few geometric primitives using Constructive Solid Geometry (CSG).

We have developed a model-oriented photogrammetric system for generic CSG models that exploits this standardization by providing a catalog from which the operator can select a specific model that he/she wants to measure. The system also comprises an interactive measurement method for parameterized CSG models, a semi-automatic fitting procedure to increase the measurement precision, and a bundle adjustment for the simultaneous estimation of the CSG parameters and the image exterior orientations. Known geometric relations within CSG models and between CSG models can be taken into account by introducing geometric constraints.

This paper focusses on the use of geometric constraints with CSG models in a photogrammetric system. The next section discusses constraints in CAD applications compared to constraints in photogrammetric applications and motivates the choice of the mathematical model. Section 3 gives a general overview of our model-oriented measurement system, while Section 4 introduces frequently used geometric constraints within an industrial installation. Section 5 explains how the exterior orientations of the images are determined in our set of test data, which is discussed in Section 6. Finally, Section 7 concludes.

2 CONSTRAINTS IN THE CONSTRUCTION AND RECONSTRUCTION OF INDUSTRIAL INSTALLATIONS

Geometric constraints in CAD applications have been subject to extensive research. Bouma et al. (2000) sees two basic strategies for constraint solving methods; instance solvers and generic solvers. Instance solvers use the explicit values of the parameters and constraints while generic solvers determine whether constraint configurations can be satisfied, independent of the values of the parameters. In their turn, instance solvers can be subdivided into analytical approaches and numerical approaches. An analytical instance solver formulates the constraints as a system of algebraic equations and uses general symbolic computations to find the solution(s). A numerical instance solver uses an iterative technique to compute a solution of the system of algebraic equations.

The use of geometric constraints in geodetic and photogrammetric applications is well known (Mikhail 1976). Constraints that are included in an iterative least-squares adjustment fall into the class of numerical instance solvers. Constraints in a least-squares adjustment can be implemented as either hard constraints or soft constraints. A hard constraint maintains a geometric relation "at all costs" while the residual of a soft constraint, in combination with a weight, is minimized in the least-squares adjustment.

The main difference between constraints in CAD applications and constraints in photogrammetric applications comes from the difference in use of the two types of applications; CAD is used in the construction phase of an object while photogrammetry is applicable to the reconstruction of an object. In the design phase, product features need to fulfill certain requirements e.g. to be parallel or perpendicular or to have a specific value, whereas during reconstruction the measured dimensions might show a slight difference from the intended values. To allow small imperfections in the constraint specification we choose to use soft constraints in our mathematical model (also known as the unified approach).

3 OVERVIEW OF PIPER

A model-oriented photogrammetric system (Piper) has been developed which allows the interactive measurement of CSG models in images. CSG models are constructed from one or more primitive shapes (such as a cylinder, a box, a sphere, etc.) that are combined using the volumetric Boolean operations union, intersection and subtraction, to construct more complex shapes. An operator selects the CSG model he/she wants to measure from a database of template models. The model is projected into the images with a so-called hidden-line projection. The hidden-line projection computes contours of curved surfaces and determines which edges, or parts of edges, are visible from the given viewpoint. The interior and exterior orientations of the images are known, or at least have approximate values.

The operator can interactively drag an edge from the hidden-line projection to the corresponding position in the image and thus perform a measurement. An observation equation is set up that directly relates the parameters of the model to the measured position. For a more detailed description of the measurement method, see Ermes et al. (1999). When a CSG model is constructed from several primitives, geometric relations often can be identified between the primitives (internal constraints). See, for example, Figure 1: a T-junction. The radii of both cylinders are equal, the cylinders are perpendicular to each other, and the beginning of the horizontal cylinder is positioned in the middle of the vertical cylinder. Integration of these relations in the interactive measurement method reduces the degrees of freedom of the two cylinders and thus facilitates the measurements. When measuring standardized components in an industrial installation, extra benefits arise because of the known dimensions of the parts.

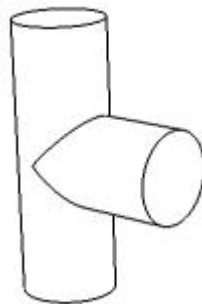


Figure 1. A hidden-line projection of a T-junction.

Not only constraints within CAD models are relevant for the reconstruction of an installation, but also geometric relations between models (external constraints) play an important role; e.g. parts can be parallel to each other, or piping

elements can be connected. The latter situation yields several constraints for the direction of the two elements and for the position of their coinciding ends. The radii of the two elements might also be equal.

The integration of internal and external constraints with the model-based measurement method has several benefits:

- Facilitates measurement. When a straight pipe is connected to an already known element, its direction and position are determined, leaving only its length to be measured.
- Enables measurement in complex situations. In industrial installations often piping elements occlude each other and are not entirely visible in the images. The application of constraints decreases the degrees of freedom of the CAD-model, which allows the reconstruction of the installation with less measurements.
- Simultaneous adjustment of adjacent models. Figure 2a shows two cylinders connected to a curved element. The transitions between the elements are smooth and only the contours give a good enough contrast for accurate measurement. The piping elements can be reconstructed by applying direction constraints and position constraints between the connections. This also means that the parameters of the different elements are correlated with each other and that a change of a parameter of one element might affect its neighboring elements. Piper can include neighboring elements in the adjustment during the interactive measurements. The operator can select the number of neighbors that will be included in the adjustment.
- Extended measuring capabilities compared to other methods. Benning (1997), Hilgers et al. (1998) and Jones et al. (1996) describe methods or systems that focus on the measurement of piping elements. For the reconstruction of curved elements these methods rely on the complete measurement of the neighboring straight cylinders. The absence of clear transitions as in Figure 2a will cause problems and in situations where two or more curves are connected to each other, as in Figure 2b, these methods will even fail. Piper combines constraints with measurements on the contours to reconstruct these elements.

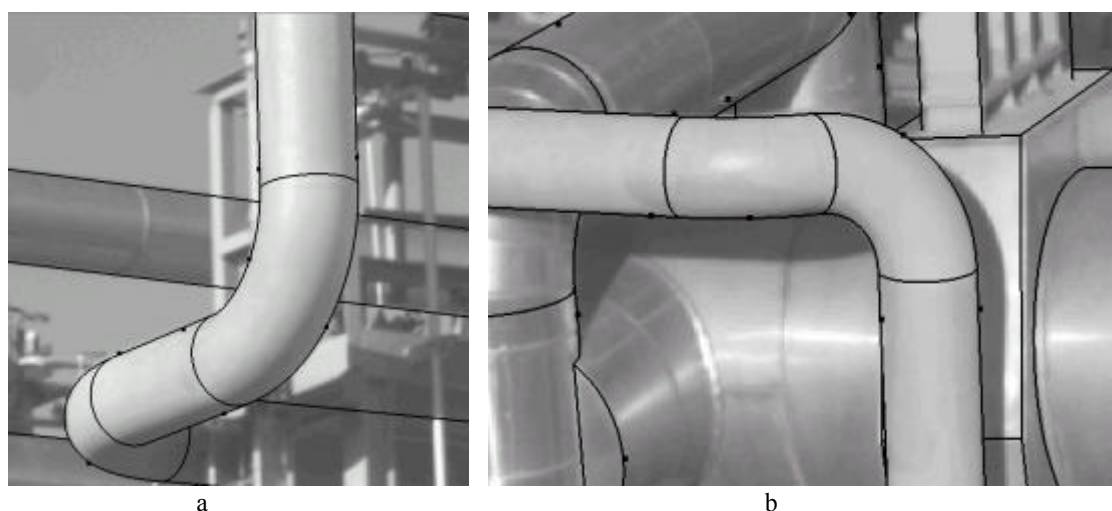


Figure 2. Examples of images of an industrial installation. The reconstructed piping elements are drawn on top using the hidden-line projection.

4 THE CONNECTION CONSTRAINTS

A set of primitive shapes is implemented within Piper. The set consists of a sphere, a cylinder, a box, a torus, a wedge, and a prism. These primitives can be combined using Boolean operations and constraints can be applied between the primitives. We will discuss two primitives (cylinder and torus) and three types of constraints (parameter, position, and direction constraints) in more detail. These primitives and constraints are used frequently in the reconstruction of industrial installations.

A cylinder, as shown in Figure 3, is constructed relative to its own coordinate system. The base of the cylinder is positioned at $(0,0,0)$, the symmetry axis coincides with the Z -axis and the top of the cylinder is located at $(L, 0, 0)$, where L is the length of the cylinder. The length together with the radius of the cylinder r , define the shape of the cylinder.

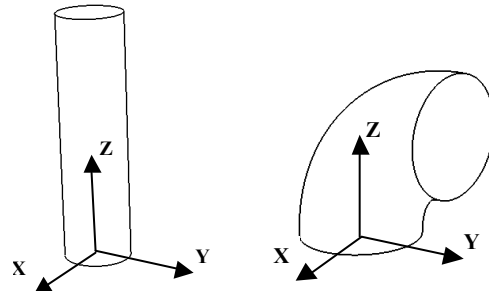


Figure 3. The cylinder and the torus with their local coordinate system.

The pose of the cylinder in object space is defined by a 3D translation \mathbf{T}_{cyl} and a 3x3 rotation matrix \mathbf{R}_{cyl} according to:

$$\mathbf{T}_{cyl} = \begin{bmatrix} x \\ y \\ z \end{bmatrix}, \mathbf{R}_{cyl} = \begin{bmatrix} \cdot & \cdot & t_1 \\ \cdot & \cdot & t_2 \\ \cdot & \cdot & t_3 \end{bmatrix} \quad (1)$$

The translation is parameterized by its three elements x , y , and z , while the rotation is parameterized by the elements t_1 , t_2 and t_3 of a 3D unit vector. Since a cylinder is symmetric around its Z-axis, the degrees of freedom concerning its rotation are reduced from 3 to 2. The rotation parameterization in (1) requires an extra constraint on the length of the vector (it must be equal to 1) but provides a representation that is free of singularities. We will refer to this rotation parameterization as a ‘trinion’. The dotted elements in the rotation matrix are not relevant for this parameterization because of the rotation symmetry in the model. When necessary they can be computed to make \mathbf{R} a valid rotation matrix.

A torus, as shown in Figure 3, has three shape parameters; a minor radius r , a major radius R , and an angle α . The base is located in its local coordinate system at $(0,0,0)$ and the curve bends towards the Y-axis. The pose of the cylinder in object space is defined by a 3D translation \mathbf{T}_{torus} and a 3x3 rotation matrix \mathbf{R}_{torus} according to:

$$\mathbf{T}_{torus} = \begin{bmatrix} x \\ y \\ z \end{bmatrix}, \mathbf{R}_{torus} = \begin{bmatrix} q_1^2 - q_2^2 - q_3^2 + q_4^2 & 2(q_1q_2 + q_3q_4) & 2(q_1q_3 - q_2q_4) \\ 2(q_1q_2 - q_3q_4) & -q_1^2 + q_2^2 - q_3^2 + q_4^2 & 2(q_2q_3 + q_1q_4) \\ 2(q_1q_3 + q_2q_4) & 2(q_2q_3 - q_1q_4) & -q_1^2 - q_2^2 + q_3^2 + q_4^2 \end{bmatrix} \quad (2)$$

The translation is parameterized by its three elements x , y , and z , while the rotation is parameterized by four quaternion elements. A 3D rotation has three degrees of freedom and, therefore, the rotation parameterization in (2) requires an extra constraint on the length of the quaternion (must equal 1) but it does provide a representation free of singularities.

When piping elements are connected to each other, continuity requirements impose constraints on the radii of the elements, the positions of both connecting ends, and the orientation of the elements. For the radii r_1 and r_2 of two elements the constraint equation is:

$$r_1 - r_2 = \varepsilon_r \quad (3)$$

Where ε_r is the residual, or difference between the two radii. For the positions \mathbf{P}_1 and \mathbf{P}_2 of two connecting ends the three constraint equations are (for x , y , and z):

$$\mathbf{P}_1 - \mathbf{P}_2 = \varepsilon_p \quad (4)$$

Where ε_p is a vector containing the residuals for the position (in x , y and z). For the directions \mathbf{D}_1 and \mathbf{D}_2 of two connecting ends, the three constraint equations are (for x , y , and z):

$$\mathbf{D}_1 + \mathbf{D}_2 = \varepsilon_d \quad (5)$$

Where ε_d is a vector containing the residuals for the direction (in x , y , and z). Constraining the direction of a connection restricts two degrees of freedom and still leaves one degree of freedom for a rotation. The use of three

constraint equations in (5) provides a formulation that is free of singularities. Note that the formulation of the direction constraint is very similar to the rotation representation of a cylinder in (1).

The constraints discussed above only give a general description; Table 1 relates these constraints to the parameters of a cylinder and a torus. The constraint equations are linearized and included as weighted observations together with the measurements in the adjustment for the model parameters. The constraint equations are weighted relative to the measurements by the operator. The weights of the measurements can be computed from the expected measurement accuracy in the images (weight $\sim 1/\text{variance}$).

	Cylinder bottom	Cylinder top	Torus bottom	Torus top
Direction	$\mathbf{R}_{cyl} \begin{bmatrix} 0 \\ 0 \\ -1 \end{bmatrix}$	$\mathbf{R}_{cyl} \begin{bmatrix} 0 \\ 0 \\ 1 \end{bmatrix}$	$\mathbf{R}_{torus} \begin{bmatrix} 0 \\ 0 \\ -1 \end{bmatrix}$	$\mathbf{R}_{torus} \begin{bmatrix} 0 \\ \sin \alpha \\ \cos \alpha \end{bmatrix}$
Position	\mathbf{T}_{cyl}	$\mathbf{T}_{cyl} + \mathbf{R}_{cyl} \begin{bmatrix} 0 \\ 0 \\ L \end{bmatrix}$	\mathbf{T}_{torus}	$\mathbf{T}_{torus} + \mathbf{R}_{torus} \begin{bmatrix} 0 \\ R(1 - \cos \alpha) \\ R \sin \alpha \end{bmatrix}$

Table 1. The directions and positions of possible connections for a cylinder and a torus, expressed in terms of their parameters.

The weights of the constraints can be related to physical properties such as the manufacturing accuracy of the part. Especially for standardized components this data is available. Connections between piping elements come in different types, such as welded connections or flanged connections. These types of connections are also standardized and, therefore, should meet accuracy requirements.

When the accuracy data is not available, the weights can be approximated by assuming a realistic accuracy. Where the position constraint is expressed in object coordinates, the direction constraint is expressed using dimensionless numbers. The weight of a direction constraint can be related to the weight of the position constraint when the effect of a change in direction is estimated in object space. For example, the maximum effect of change in direction of a cylinder is its length or its radius, whichever is biggest. Multiplying the weight of the position constraint by the squared size of a model for the weight of the direction constraint produces ‘resistance’ in object space the same order of magnitude for both constraints. Note that the expressions in Table 1 for the positions contain rotation parameters that are also multiplied by shape parameters thus producing the same result in the adjustment as the weighting described above.

A third method for the computation of the weights is Variance Components Estimation (VCE) (Luhmann, 2000). VCE is a statistical technique and is applicable when a large number of redundant measurements and constraints are available. By dividing the measurements and constraints into two groups (components) the residuals of both groups can be analyzed and the variance of both groups can be estimated. The group of constraints can even be further divided into groups of different constraint types to estimate the weights of the different types.

5 BUNDLE ADJUSTMENT

Piper also contains functionality for estimating the exterior orientations of the images, this estimation was used in the experiment described in the next section. So far, we used the measurement method described in Ermes et al. (1999) for estimating the pose and shape of CSG models assuming known camera orientations. However, the camera orientations can also be estimated using the same measurements and this avoids a separate triangulation stage for obtaining the camera orientations. A point on an edge of a model \mathbf{p}_e is backprojected into the image at point \mathbf{p}_i according to:

$$\mathbf{p}_i = \mathbf{T}_i \mathbf{T}_e \mathbf{T}_o \mathbf{p}_e \quad (6)$$

Where \mathbf{T}_o denotes the pose of the model in object coordinates, \mathbf{T}_e denotes the pose of the object space in camera coordinates (the inverse of the exterior orientation), and \mathbf{T}_i is the interior orientation of the camera. The linearized observation equations as discussed in Ermes et al. (1999), are extended with the partial derivatives of the parameters of \mathbf{T}_e , which is parameterized with a translation and a quaternion.

The simultaneous estimation of the exterior orientations and the pose and shape of the models changes the workflow compared to the separate triangulation and model-measuring stages. In the pilot project described in the next section we choose a distinct model from which at least one dimension was known. The pose of the model and the dimension are set to specific values so that the model is positioned in object space with a known scale.

The exterior orientation of an image containing this model can now be estimated. An operator provides an approximate value for the orientation, either by entering the numeric values of the orientation, or by interactively choosing a viewpoint in a 3D viewer (like a VRML browser). In this viewer, the image is projected in the background while the models are displayed using a hidden-line projection. Starting with the approximate orientation, the operator makes more precise measurements on the displayed model. Using these measurements, an accurate estimate of the exterior orientation is computed. This is done for all the images that show the selected model. Other models can be measured using this set of images which gives the opportunity to orient more images that show these newly measured models. After which more images can be included in the measurements, and so on. Once all the measurements are complete, a global bundle adjustment is computed in which all model parameters and exterior orientations are estimated.

This method uses parameterized CSG models as the connecting entities between images in contrast to the use of points in a triangulation-based bundle adjustment.

6 EXPERIMENTS

A pilot project was undertaken at a gas exploration site of the NAM in Tjuchem, the Netherlands. The recorded area comprises a gas-drying unit, which measures about 30x30 square meters and has a maximum height of about 5 meters. In about 3 hours 102 images were recorded on site using a Kodak DCS420 camera (1012x1524 pixels). See the images in Figure 4 for an overview of the installation. The interior orientation and lens distortion of the camera are known. Several dimensions of the installation, such as radii and lengths of piping elements, were tape-measured.

The exterior orientations were obtained using the model-based bundle adjustment described above. The measurements started with the large box in the foreground of Figure 4a. The orientation of the box in the object coordinate system is constrained so that one corner of the box coincides with the origin and the box is aligned with the object coordinate axes. The length of the box (10645mm) was measured using a steel tape and the size of the model was constrained to that value. Starting with the box, all the images that show this model could be oriented. After that the procedure described in the previous section was followed.



Figure 4. Images of the gas-drying unit.

Only some (36) of the recorded images were used for the measurements. The installation was modeled using 218 CSG models, which were built with a total of 288 geometric primitives. Figure 5 shows the reconstructed model. The primitives and the image orientations are parameterized with a total of 2706 parameters. The operator measured 2744 points on model edges and applied 1487 constraints. 313 extra constraints were included for constraining the lengths of the rotation-parameter vectors, giving a total of 4544 observation equations.

The measurements took approximately 2 weeks, although one must keep in mind that the current application is a first prototype. Improvements to the user interface can still be made to increase the efficiency of the process. Assuming an accuracy of 1 pixel of the measurements by the operator, the estimated accuracy in object space is approximately 5-

10mm. We checked the remaining tape measurements against the photogrammetrically obtained model dimensions and the differences were all less than the estimated accuracy.

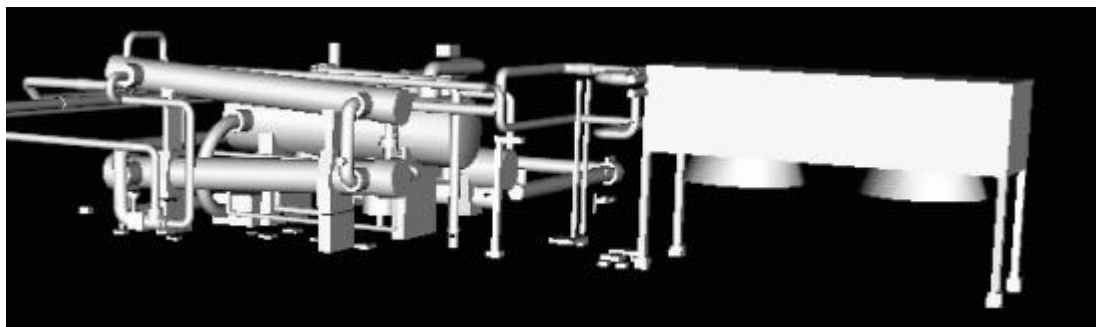


Figure 5. The reconstructed model.

7 CONCLUSIONS

We implemented a model-based photogrammetric system in combination with geometric constraints and a bundle adjustment. The unique feature of this system is that measurements on the back-projected model edges are directly related to the parameters of the CSG model and the parameters of the image orientation.

The integrated bundle adjustment overrides the need for a separate triangulation stage and no markers need be attached to the installation. Instead, a one-step procedure, in which the installation is measured and the image orientations are determined, is presented.

Geometric constraints between the primitives of a CSG model and geometric constraints between different CSG models are included in the least-squares estimation of the parameters as weighted linearized observation equations.

The model-based photogrammetric system, including the geometric constraints and the bundle adjustment, is successfully applied for the reconstruction of a complex industrial installation.

ACKNOWLEDGMENTS

We would like to thank the NAM for their cooperation during the pilot project.

This research is supported by the Dutch Technology Foundation (STW).

REFERENCES

- Benning, W., 1997. PHIDIAS-MS – Eine Digitale Photogrammetrieapplication unter MicroStation für Nahbereichsanwendungen. *Allgemeine Vermessungsnachrichten*, pp. 16-25.
- Bouma, W., Chen, X., Fudos, I., Hoffmann, C., Vermeer, P.J., An Electronic Primer on Geometric Constraint Solving. <http://www.cs.purdue.edu/homes/cmh/electrobook/intro.html> (March 2000).
- Ermes, P., van den Heuvel, F.A., Vosselman, G., 1999. A Photogrammetric Measurement Method Using CSG Models. *International Archives of Photogrammetry and Remote Sensing*, Vol 32, Part 5W11, Thessaloniki, pp. 36-42.
- Hilgers, G., Przybilla, H.-J., Woytowics, D., 1998. The Digital Photogrammetric Evaluation System PHAUST for As-Built Documentation. *International Archives of Photogrammetry and Remote Sensing*, Vol 32, Part 5, Hakodate, pp. 226-229.
- Jones, M.A., Chapman, D.P., Hamid, A.A., Deacon, A.T.D., 1996. Close Range Photogrammetry Using Geometrical Primitives for Efficient CAD Modelling of Industrial Plant. *International Archives of Photogrammetry and Remote Sensing*, Vol 31, Part B5, Vienna.
- Luhmann, T., 2000. *Nahbereichsphotogrammetrie*. Wichmann, Heidelberg, pp. 67-68.
- Mikhail, E.M., 1976. *Observations and Least Squares*. Dun-Donnelley, New York.